

Article

Synthesis and Structural Studies of Complexes of Bis(pentafluorophenyl)mercury with Di(phosphane oxide) Ligands

Shalini Rangarajan ¹, Owen A. Beaumont ², Zhifang Guo ², Maravanji S. Balakrishna ¹, Glen B. Deacon ² 
and Victoria L. Blair ^{2,*} ¹ IITB-Monash Academy, Indian Institute of Technology, Bombay 400076, India² School of Chemistry, Monash University, Melbourne 3800, Australia

* Correspondence: victoria.blair@monash.edu.au

Abstract: The reaction of bis(pentafluorophenyl)mercury with the ligands bis(diphenylphosphano) methane P,P'-dioxide ($(\text{Ph}_2\text{P}(\text{O}))_2\text{CH}_2$) (**1**), bis[2-(N,N,N',N'-tetraethylaminophosphano) imidazol-1-yl] methane P,P'-dioxide ($(2\text{-PO}(\text{NEt}_2)_2\text{C}_3\text{N}_2\text{H}_2)_2\text{CH}_2$) (**2**) and bis (2-diphenylphosphanophenyl) ether P,P'-dioxide ($(2\text{-PPh}_2(\text{O})\text{C}_6\text{H}_4)_2\text{O}$) (**3**) afforded crystalline σ -donor complexes $[\{\text{Hg}(\text{C}_6\text{F}_5)_2\}_2\{\text{Ph}_2\text{P}(\text{O})\}_2\text{CH}_2]$ (**1Hg**), $[\text{Hg}(\text{C}_6\text{F}_5)_2\{2\text{-PO}(\text{NEt}_2)_2\text{C}_3\text{N}_2\text{H}_2\}_2\text{CH}_2]_n$ (**2Hg**) and $[\text{Hg}(\text{C}_6\text{F}_5)_2\{2\text{-PPh}_2(\text{O})\text{C}_6\text{H}_4\}_2\text{O}]$ (**3Hg**), respectively. The molecular structures of **1Hg**, **2Hg** and **3Hg** show considerable differences. In complex **1Hg**, a single bridging bidentate ligand connects two three-coordinate T-shape mercury atoms with a near linear C-Hg-C atom array. Complex **2Hg** is a one-dimensional coordination polymer in which adjacent four-coordinate mercury atoms with a linear C-Hg-C atom array are linked by bridging bidentate O,O'- ligands, whilst in complex **3Hg** a T-shape three-coordinate mercury atom is ligated by (**3**) in a monodentate fashion. The Hg-O bond lengths of complexes **1Hg**, **2Hg** and **3Hg** differ substantially (range 2.5373(14)–2.966(3) Å) owing to structural and bonding differences.

Keywords: phosphane oxide; bis(pentafluorophenyl)mercury; P=O group coordination; T-shape three coordination; novel-shaped four coordination



Citation: Rangarajan, S.; Beaumont, O.A.; Guo, Z.; Balakrishna, M.S.; Deacon, G.B.; Blair, V.L. Synthesis and Structural Studies of Complexes of Bis(pentafluorophenyl)mercury with Di(phosphane oxide) Ligands. *Crystals* **2023**, *13*, 530. <https://doi.org/10.3390/cryst13030530>

Academic Editors: Priya Ranjan Sahoo, Clara Gomes and Akbar Bakhtiari

Received: 21 February 2023

Revised: 9 March 2023

Accepted: 16 March 2023

Published: 20 March 2023



Copyright: © 2023 by the authors. Licensee MDPI, Basel, Switzerland. This article is an open access article distributed under the terms and conditions of the Creative Commons Attribution (CC BY) license (<https://creativecommons.org/licenses/by/4.0/>).

1. Introduction

Di(aryl)mercury compounds, HgR_2 , have a stable C-Hg-C arrangement in their structures and show virtually no Lewis acidity and it is a major challenge to enhance the acceptor properties. However, the early success in the synthesis of complexes between bis(pentafluorophenyl) mercury and ligands such as 2,2-bipyridine (bpy) and 1,2-bis(diphenylphosphano)ethane (dppe) [1] showed that the lack of Lewis acidic character shown by diphenylmercury [1–4] can be overcome by fluorine substitution. However, neither methylpentafluorophenyl- nor pentafluorophenyl(phenyl)-mercury would form similar complexes [1]. Both $[\text{Hg}(\text{C}_6\text{F}_5)_2\text{L}]$ (L = bpy or dppe) and $[\text{Hg}(\text{C}_6\text{F}_5)_2\text{phen}]$ (phen = 1,10-phenanthroline, Chart 1, I) were later prepared by thermal decarboxylation of the corresponding pentafluorobenzoatomercury precursors, $[\text{Hg}(\text{O}_2\text{CC}_6\text{F}_5)_2\text{L}]$ [5]. A wider range of $[\text{Hg}(\text{C}_6\text{F}_5)_2\text{L}]$ complexes, where for example L = methyl-substituted 2,2'-bipyridine and 1,10-phenanthroline, 2,2'-biquinoline, ethane-1,2-diamine (en), PPh_3 , PPh_3O , together with $[\{\text{Hg}(\text{C}_6\text{F}_5)_2\}_2\text{L}]$ L = $(\text{EPh}_2)_2\text{CH}_2$ (E = P or As) were prepared (Chart 1, II), but a study of their molecular weights in benzene and chloroform by osmometry showed most were substantially dissociated in solution into $\text{Hg}(\text{C}_6\text{F}_5)_2 + \text{L}$, with only phen and en complexes showing significant stability [6]. Determination of the molecular structure of $[\text{Hg}(\text{C}_6\text{F}_5)_2\}_2(\text{AsPh}_2(\text{CH}_2)\text{AsPh}_2)]$ [7] showed the diarsane ligand bridging two three-coordinate (T-shape) mercury atoms, where the Hg-As distance is only 0.3 Å less than the sum of the van der Waals radii of arsenic and mercury with a conservative value of 1.73 Å for mercury (Chart 1, III) [8]. Naumann et al. showed that halide ions can coordinate to

give species of the type $[\text{Hg}(\text{C}_6\text{F}_5)_2\text{X}]^-$ ($\text{X} = \text{Cl}, \text{Br}$ and I) which were crystallized using bulky cations such as PPh_4^+ and $[\text{K}(18\text{-crown-6})]^+$ [9] (Chart 1, IV). These compounds are three-coordinate systems adopting a T-shape geometry. Later, the same group isolated trinuclear complexes $[\{\text{Hg}(\text{C}_6\text{F}_5)_2\}_3\text{X}]^-$ ($\text{X} = \text{Cl}, \text{Br}, \text{I}$), also utilizing bulky cations (Chart 1, V) [10]. Besides these complexes with σ -donors, a few π -donor complexes with arenes [11,12] (e.g., Chart 1, VI, VII) and transition metal Schiff base derivatives [13,14] have been obtained. Complexes with metallophilic interactions, e.g., $\text{Au}^{\text{I}}\text{-Hg}^{\text{II}}$ [15,16] are also known. It is striking that despite a considerable amount of investigation, structural information on complexes of $[\text{Hg}(\text{C}_6\text{F}_5)_2]$ containing neutral σ donors is limited to the one complex $[\{\text{Hg}(\text{C}_6\text{F}_5)_2\}_2(\text{AsPh}_2\text{CH}_2\text{AsPh}_2)]$ (Chart 1, III).

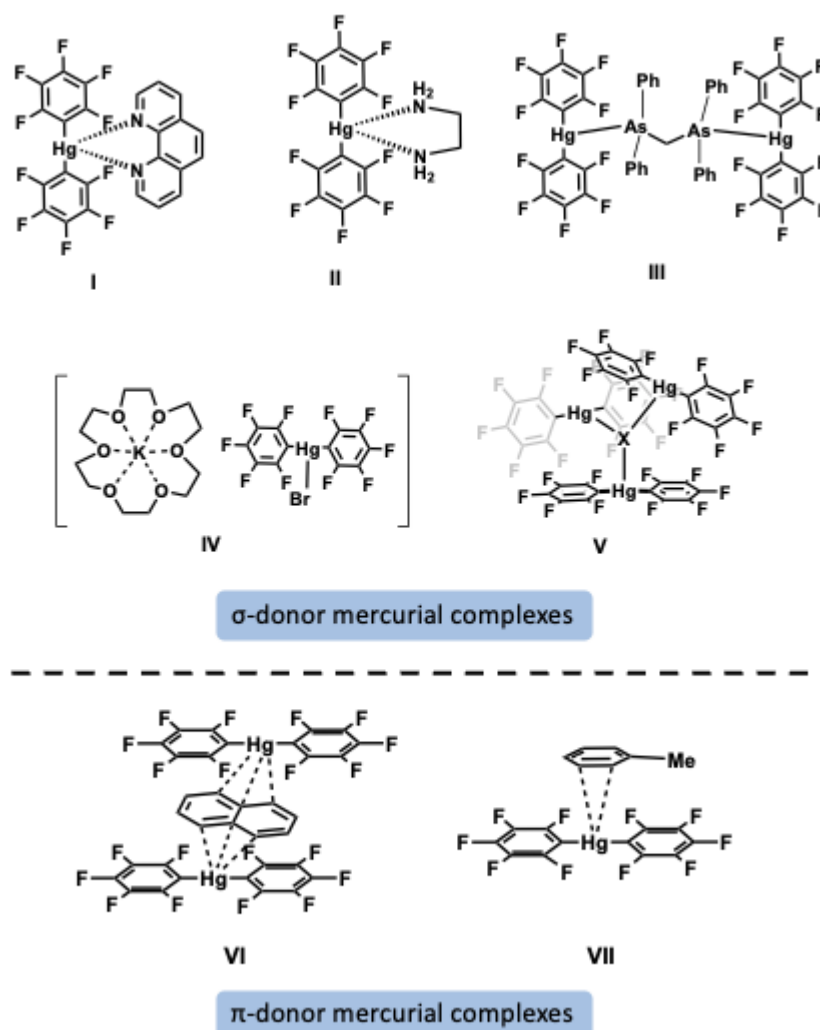


Chart 1. Selected complexes of bis(pentafluorophenyl)mercury(II) with σ - and π -donor moieties I [6], II [6], III [7], IV [9], V [10], VI [11] and VII [12].

In order to obtain crystalline coordination derivatives of bis(pentafluorophenyl)mercury, we have examined complexation with three bulky, potentially chelating, bis(phosphane oxide) ligands, namely bis (diphenylphosphano)methane $\text{P,P}'$ -dioxide (**1**), bis(2-(N,N,N',N' -tetraethyl-diaminophosphano)imidazol-1-yl)methane $\text{P,P}'$ -dioxide (**2**) and bis(2-diphenylphosphanophenyl) ether $\text{P,P}'$ -dioxide (**3**) (Chart 2).

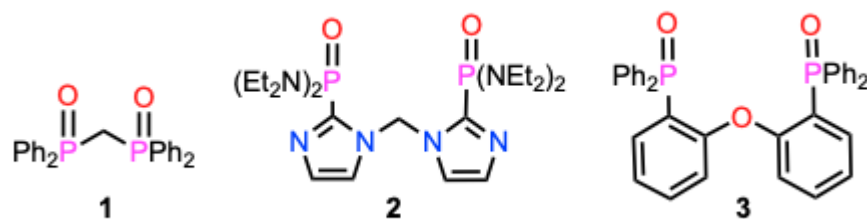


Chart 2. Bis(phosphane oxide) ligands used in this study.

We were encouraged by recent studies of phosphane-oxide coordination to several mercury, especially organomercury, acceptors (Chart 3) [17–21]. The choice of ligands was also influenced by the spear-like $\text{P}=\text{O}$ donor, which reduces steric repulsion close to the metal compared to tetraaryldiphosphane or diarsane ligands (Chart 1, III), whilst still retaining more distant bulk to aid crystallization. The favorable polarity, P^+-O^- of the phosphoryl group, and the possibility of a chelate effect was also considered. Representative complexes have now been synthesized and structurally characterized resulting in different types of ligation and considerable variation in the $\text{Hg}-\text{O}$ bond lengths.

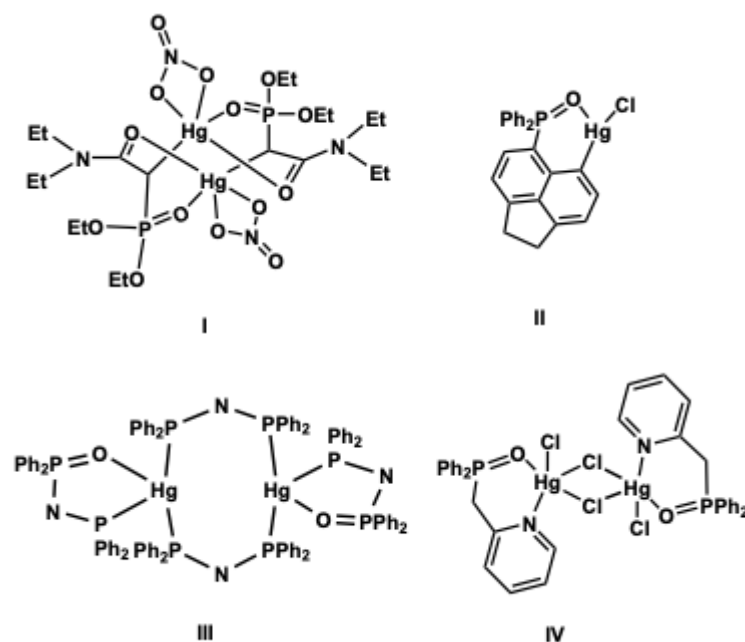
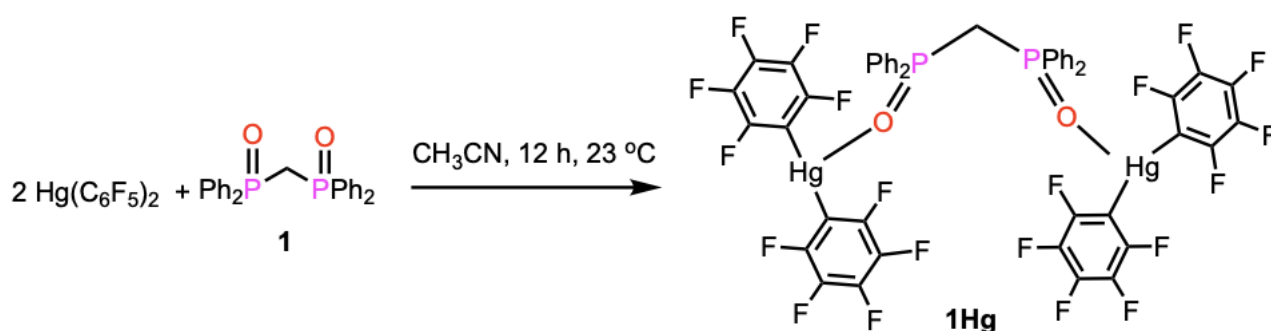


Chart 3. Selected mercurial complexes I [17], II [19], III [20] and IV [21] with different phosphane oxide groups.

2. Results and Discussion

2.1. Synthesis of $[\{\text{Hg}(\text{C}_6\text{F}_5)_2\}_2\{\text{Ph}_2\text{P}(\text{O})\}_2\text{CH}_2]$ (**1Hg**)

The bisphosphane oxide $\{\text{Ph}_2\text{P}(\text{O})\}_2\text{CH}_2$ (**1**) was synthesized by the oxidation of bis(diphenylphosphino)methane with H_2O_2 [22]. The reaction of **1** with $\text{Hg}(\text{C}_6\text{F}_5)_2$ in a 1:2 mole ratio in acetonitrile resulted in the formation of the dimercury complex $[\{\text{Hg}(\text{C}_6\text{F}_5)_2\}_2\{\text{Ph}_2\text{P}(\text{O})\}_2\text{CH}_2]$ **1Hg** in which **1** acts as a bridge (Scheme 1).



Scheme 1. Synthesis of $[\{\text{Hg}(\text{C}_6\text{F}_5)_2\}_2\{\text{Ph}_2\text{P}(\text{O})\}_2\text{CH}_2]$ (**1Hg**).

Slow evaporation of an acetonitrile solution of complex **1Hg** yielded a crop of colorless crystal blocks. The same reaction carried out on a 1:1 mole ratio also gave rise to **1Hg**, indicating a preference for the bridging coordination of **1**. The bulk composition of **1Hg** was established by elemental analysis. The $^{19}\text{F}\{^1\text{H}\}$ and $^{31}\text{P}\{^1\text{H}\}$ NMR spectra are very similar to those of the reactants [22,23] (see ESI, Figures S1 and S2). The IR spectrum of **1Hg** revealed a strong $\nu(\text{P}=\text{O})$ band at 1181 cm^{-1} (see ESI, Figure S3), somewhat displaced to longer wavelengths from the absorptions of the free ligand ($1212, 1197, 1176\text{ cm}^{-1}$) [24] as expected due to the coordination of a $\text{P}=\text{O}$ group [25]. Of further interest is that the ‘X-sensitive’ mode involving C-Hg stretching of the HgC_6F_5 group is shifted from 812 cm^{-1} in $\text{Hg}(\text{C}_6\text{F}_5)_2$ [5] to 794 cm^{-1} in the spectrum of complex **1Hg** in a direction consistent with weakening the Hg-C bond on coordination. Carbon-fluorine stretching is observed at 1055 and 957 cm^{-1} .

2.2. Molecular Structure of $[\{\text{Hg}(\text{C}_6\text{F}_5)_2\}_2\{\text{Ph}_2\text{P}(\text{O})\}_2\text{CH}_2]$ (**1Hg**)

The compound **1Hg** crystallizes in the monoclinic space group $\text{C}2/c$ (Figure 1). The coordination geometry of the mercury atoms is a distorted T-shape, where the O-Hg-C angles are $86.56(7)^\circ$ and $97.38(6)^\circ$ (Figure 1). The C-Hg-C angle ($175.06(9)^\circ$) is reduced slightly compared to that in $\text{Hg}(\text{C}_6\text{F}_5)_2$ ($179.1(5)^\circ$ original rotamer; $177.10(11)^\circ$ new rotamer) [26], as a result of O-Hg bonding. However, the Hg-C bond lengths ($2.063(2), 2.071(2)\text{ \AA}$) are not significantly affected when compared with $\text{Hg}(\text{C}_6\text{F}_5)_2$ ($2.076(11), 2.066(11)\text{ \AA}$ original rotamer; $2.064(3), 2.065(3)\text{ \AA}$ new rotamer) [26]. The Hg-O bond length ($2.5373(14)\text{ \AA}$) is much shorter than the sum (3.23 \AA) of the van der Waals radii of mercury and oxygen [8,27]. In addition, the Hg-O bond length of **1Hg** is close to values observed for Hg-O in **II** (2.545 \AA), **III** ($2.624(3)\text{ \AA}$) and **IV** ($2.510(2)\text{ \AA}$) (Chart 3), where Hg-O bonding is assisted by chelation, while **II** and **IV** (Chart 3) have arylmercuric chlorides as the acceptors, which are normally stronger Lewis acids than diarylmercurials. The most convincing comparison is the similarity with Hg-O of **II** (Chart 3) which has the same coordination number as **1Hg**. The stereochemistry of the mercury atom is explicable in terms of linear sp hybridization to provide the acceptor orbitals for the pentafluorophenyl groups leaving a weaker acceptor p orbital normal to the sp axis for the oxygen donor atom. The $\text{P}=\text{O}$ and $\text{P}-\text{C}$ bond lengths (Figure 1) are close to those ($1.486(2)\text{ \AA}$ -and $1.815(2)\text{ \AA}$, respectively) of the ligand **1** [28], hence coordination does not greatly affect the ligand structure. Examination of the supramolecular interactions in **1Hg** show $\text{C}-\text{H}\cdots\text{F}-\text{C}$ bonds and displaced $\pi\cdots\pi$ interactions along with intermolecular $\text{C}\cdots\text{F}$ contacts (see ESI, Figures S4–S6). The $\text{CH}\cdots\text{FC}$ interactions ($2.471\text{--}2.496\text{ \AA}$) (Table 1) are less than 2.55 \AA considered to be the limit of effectiveness for such interactions [29], and the offset $\pi\cdots\pi$ interactions (3.384 \AA), are shorter than the sum of the van der Waals radii of two aromatic rings (3.5 \AA) [30]. The $\text{C}\cdots\text{F}$ contacts ($3.007\text{--}3.64\text{ \AA}$) (see ESI, Table S1) lie near the sum of the van der Waals radii of C and F [27] and perhaps represent non-bonding/steric limits.

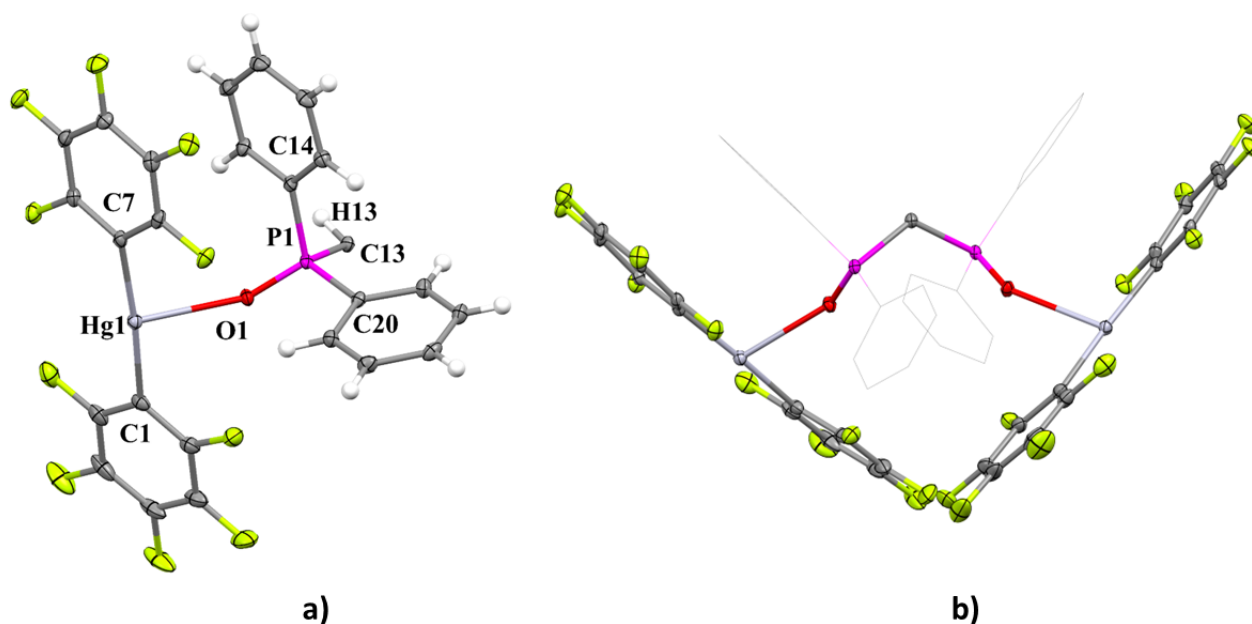


Figure 1. Molecular structure of **1Hg** (a) asymmetric unit and (b) perspective view of the complex. All hydrogen atoms are omitted for clarity. Displacement ellipsoids are drawn at the 30% probability level. Selected bond lengths (Å) and bond angles (°): Hg1–O1 2.5373(14), P1–O1 1.4895(15) P1–C13 1.8121(15), P1–C14 1.810(2), P1–C20 1.796(2). Hg1–C1 2.063(2), Hg1–C7 2.071(2), C1–Hg–C7 175.06 (9), O1–Hg1–C7 86.56(7), O1–Hg1–C1 97.38(6), P1–C13–P1' 120.42(16).

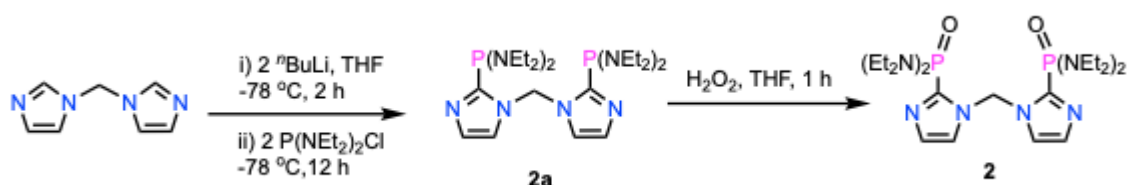
Table 1. Hydrogen-bond geometry of **1Hg** (Å, °).

<i>D</i> –H··· <i>A</i>	<i>D</i> –H	H··· <i>A</i>	<i>D</i> ··· <i>A</i>	<i>D</i> –H··· <i>A</i>
C15–H15···F6 ^[i]	0.96	2.496	3.164	127
C13–H13···F3 ^[ii]	0.95	2.471	3.398	176

^[i] $-x, y, 1.5-z$ and ^[ii] $1-x, y, 1.5-z$.

2.3. Synthesis of {2-*PO*(NEt₂)₂C₃N₂H₂}₂CH₂ (**2**)

Bis[2-(*N,N,N',N'*-tetraethylidiaminophosphano)imidazol-1-yl]methane (**2a**) was prepared by a slight modification of the reported procedure [31,32]. Bis(imidazol-1-yl)methane was treated with two equivalents of ⁿBuLi in tetrahydrofuran at -78 °C followed by the addition of two equivalents of P(NEt₂)₂Cl. The reaction mixture containing compound **2a** was observed in the ³¹P{¹H} NMR spectrum with a peak at 67.3 ppm (see ESI, Figure S7), and was oxidized to bis[2-(*N,N,N',N'*-tetraethylidiamino)phosphano)imidazol-1-yl]methane P,P'-dioxide **2** using H₂O₂ (Scheme 2), identified by ¹H and ³¹P{¹H} NMR spectroscopy and X-ray crystallography. The methylene protons of **2** appear at 8.05 ppm in the ¹H NMR spectrum and are in the range similar to analogous reported di(phosphane) oxides (7.12–8.06 ppm, mainly overlapping with Ph-group resonances, which are not present in **2**) [33]. The ³¹P{¹H} NMR spectrum of **2** shows a single resonance at 16.0 ppm (see ESI, Figures S8 and S9) and the IR contains strong peaks at (1220–1202) cm⁻¹ corresponding to the ν(P = O) band (see ESI, Figure S11).



Scheme 2. Synthesis of ligand **2**.

2.4. Molecular Structure of $\{2\text{-PO}(\text{NEt}_2)_2\text{C}_3\text{N}_2\text{H}_2\}_2\text{CH}_2$ (**2**)

Single crystals of **2** suitable for single crystal X-ray analysis were obtained from a hexane solution of **2** kept at $-20\text{ }^\circ\text{C}$ for 24 h. The phosphane oxide **2** crystallizes in the monoclinic space group $\text{P2}_1/\text{n}$ (Figure 2). The phosphorus atoms have a distorted tetrahedral geometry with the bond angles ranging from $110.07(10)^\circ$ – $119.81(13)^\circ$ (Figure 2). This spread of angles is much greater than observed ($111.43(6)$ – 113.10°) for an analogous ligand in which phenyl groups replace the NEt_2 groups of **2**, namely $\text{CH}_2(1,2\text{-C}_3\text{H}_2\text{N}_2\text{PPh}_2\text{O})_2$ [33], presumably owing to the greater steric effect of the NEt_2 moiety. However, the variation of angles is increased for the phenyl-substituted ligand if the imidazole moiety is replaced by a triazole unit [33]. The $\text{P}=\text{O}$ bond distances are in the range $1.4773(11)$ – $1.4783(11)\text{ \AA}$, and are marginally shorter than in the phenyl-substituted analogue above ($1.4854(10)$ – $1.4881(10)\text{ \AA}$ [33]). This may seem counter-intuitive given that phenyl groups are electron withdrawing and NEt_2 electron donating. The molecular structure of **2** further shows the presence of the following intermolecular interactions in ligand **2**: $\text{C-H}\cdots\text{C-H}$, $\text{C-H}\cdots\text{O}$ interactions and $\text{H}\cdots\text{H}$ contacts (Table 2; see also ESI, Figure S12).

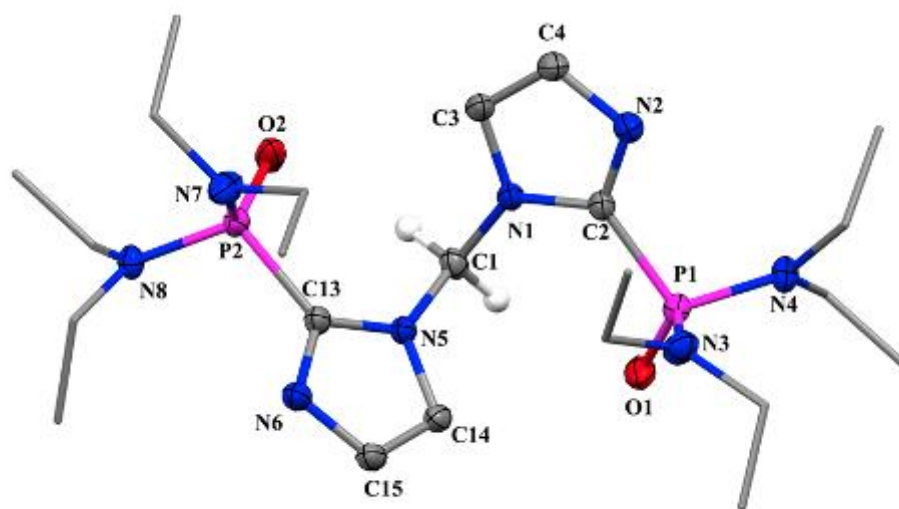


Figure 2. Molecular structure of **2**. All hydrogen atoms except CH and lattice acetonitrile are omitted for clarity. Displacement ellipsoids are drawn at the 30% probability level. Selected bond lengths (\AA) and bond angles ($^\circ$): P1-O1 $1.4773(11)$, P2-O2 $1.4783(11)$, P1-N3 $1.6373(13)$, P1-N4 $1.6407(11)$, P2-N7 $1.6444(15)$, P2-N8 $1.6339(11)$, P1-C2 $1.8056(12)$, P2-C13 $1.8025(12)$, C1-N1 $1.4589(16)$, C1-N5 $1.4618(16)$, N5-C1-N1 $112.10(11)$, O1-P1-N3 $117.86(7)$, O1-P1-N4 $110.42(6)$, O1-P1-C2 $110.31(6)$, O2-P2-N8 $110.79(6)$, O2-P2-N7 $119.71(8)$, O2-P2-C13 $110.07(6)$.

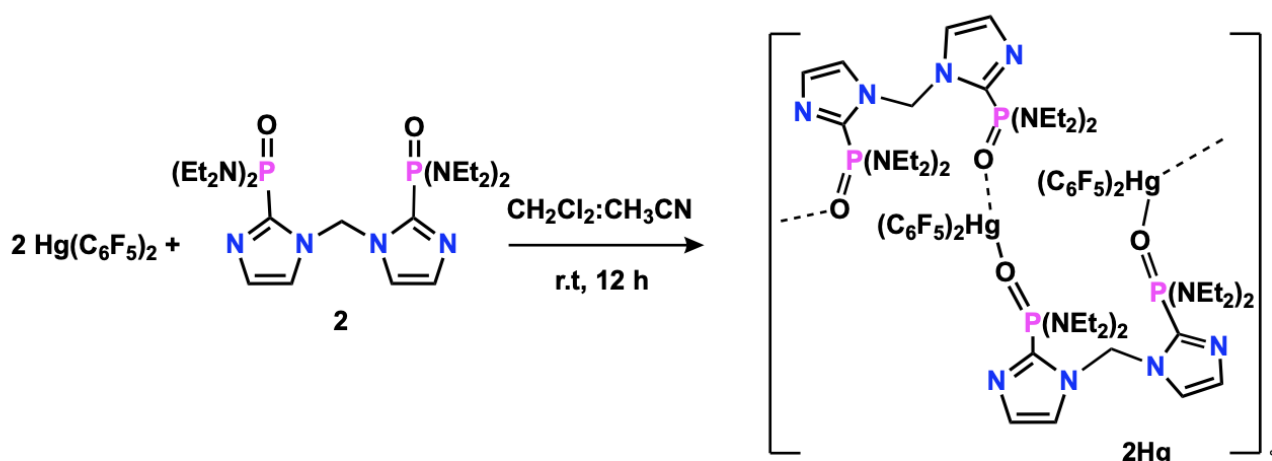
Table 2. Hydrogen-bonds geometry (\AA , $^\circ$) of **2**.

D–H \cdots A	D–H	H \cdots A	D \cdots A	D–H \cdots A
$\text{C22-H22B}\cdots\text{C3}$ [i]	0.97	2.789	3.651	148
$\text{C1-H1B}\cdots\text{O2}$ [ii]	0.97	2.642	3.412	137

[i] x,y,z and [ii] x,y,z .

2.5. Synthesis of $[\text{Hg}(\text{C}_6\text{F}_5)_2\{2\text{-PO}(\text{NEt}_2)_2\text{C}_3\text{N}_2\text{H}_2\}_2\text{CH}_2]_n$ (**2Hg**)

Treatment of phosphane oxide **2** with $\text{Hg}(\text{C}_6\text{F}_5)_2$ in a 1:2 mole ratio (Scheme 3) followed by a slow evaporation of the solution yielded the 1D-coordination polymer **2Hg** as colorless blocks.



Scheme 3. Synthesis of complex **2Hg**.

2.6. Structure of $[\text{Hg}(\text{C}_6\text{F}_5)_2\{2\text{-PO}(\text{NEt}_2)_2\text{C}_3\text{N}_2\text{H}_2\}_2\text{CH}_2]_n$ (**2Hg**)

Complex **2Hg** crystallizes in the triclinic space group P-1 and has a polymeric form (Figure 3), in which **2** acts as an O, O' bridging bidentate ligand between adjacent mercury atoms. Each mercury is four-coordinate with linear C-Hg-C units adding two oxygen donor atoms approximately normal to the C-Hg-C spine. The donor atoms can be envisaged as occupying the axial and two adjacent equatorial positions of an octahedron, i.e., with two adjacent equatorial positions empty. The stereochemistry is essentially as expected for two sp hybrid orbitals on mercury accommodating the C_6F_5 lone pairs and two p orbitals used for the P = O lone pairs. The Hg-C bond lengths of $\text{Hg}(\text{C}_6\text{F}_5)_2$ are essentially unchanged on coordination whilst the C-Hg-C angle has opened slightly to exactly linear from that of the free mercurial ($179.1(5)^\circ$ original rotamer; $177.10(11)^\circ$ new rotamer) [26]. The Hg-O bond lengths (2.966(3), 2.979(4) Å) are ca. 0.025 Å within the sum of the van der Waals radii of Hg and O [8,27], but are much longer than in **1Hg**, partly owing to the higher coordination number of mercury in **2Hg** than **1Hg**. These values are slightly longer than Hg-O (2.824(4)–2.895(4) Å) of the complex of $(\text{Me}_2\text{N})_3\text{P}=\text{O}$ with the cyclic trimeric mercurial complex $[\text{Hg}(o\text{-C}_6\text{F}_4)]_3$ [18]. The P-O bond lengths are $\sim 1.475(4)$ – $1.479(4)$ Å with not much change with respect to the ligand **2**.

Further examination of the molecular structure of **2Hg** revealed C-H \cdots N-C, C-H \cdots F-C, C-H \cdots C and C-H \cdots N interactions along with intermolecular F-C \cdots C and H \cdots H contacts (Table 3; see also ESI, Figures S13–S17). The C-H \cdots F-C interactions are between 2.373–2.438 Å, less than 2.55 Å which is considered to be the limit for such interactions to be significant [29] and the C-H \cdots N-C interaction is 2.693 Å which is in the reported range [34] (see ESI, Table S3).

Table 3. Hydrogen-bond geometry (Å, °) of **2Hg**. Cg1 is C30-C35.

D-H \cdots A	D-H	H \cdots A	D \cdots A	D-H \cdots A
C43-H43A \cdots F1 [i]	0.96	2.438	3.365	162
C23-H23B \cdots F2 [iii]	0.96	2.373	3.261	154
C10-H10B \cdots Cg1 [iii]	0.97	3.043	3.831	139.3
C22A-H22A \cdots N6 [iv]	0.97	2.693	3.492	140

[i] x,y,z [ii] x,y,z [iii] 1-x,1-y,1-z [iv] x,y,z.

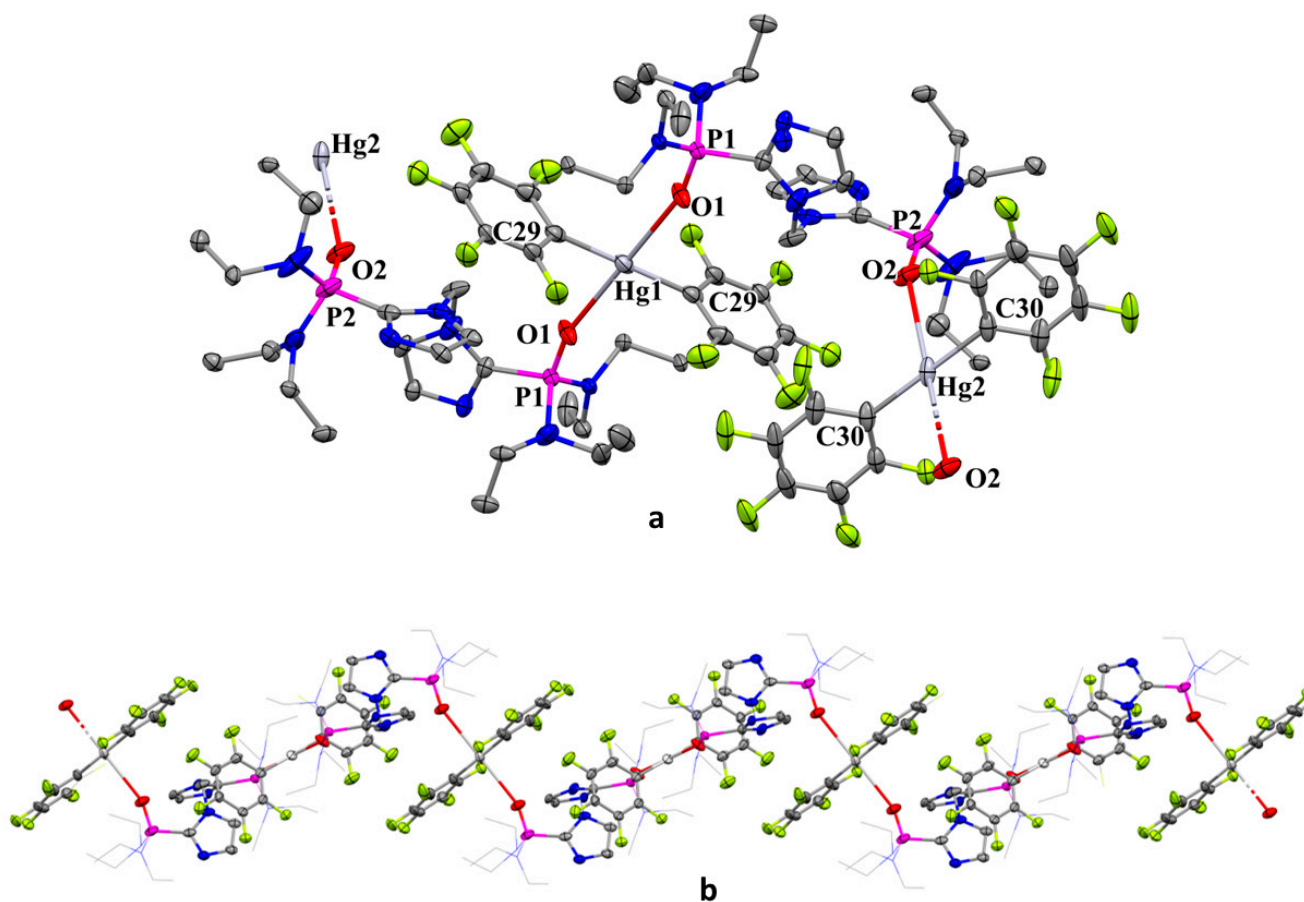
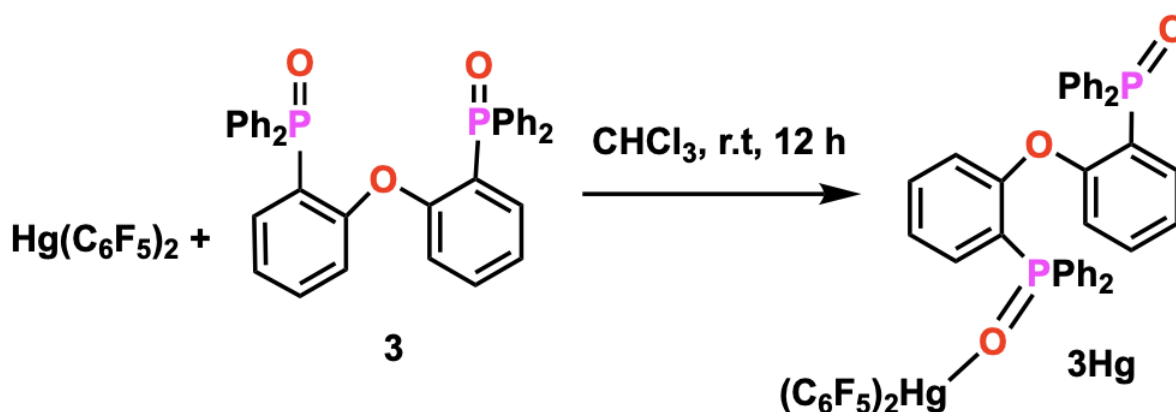


Figure 3. Molecular structure of **2Hg** (a) asymmetric unit and (b) perspective view of 1D polymer. Selected bond lengths (Å) and bond angles (°): Hg1-O1 2.966(3), Hg2-O2 2.979(4), P1-O1 1.475(3), P2-O2 1.479(4), Hg1-C29 2.061(5), Hg2-C30 2.055(5), C29-Hg1-O1 92.77(14), C30-Hg2-O2 82.05(18), C30'-Hg2-O2 97.95(18), C29'-Hg1-C29 180.0, C30'-Hg2-C30 180.0.

2.7. Synthesis of $[\text{Hg}(\text{C}_6\text{F}_5)_2\{2\text{-PPh}_2(\text{O})\text{C}_6\text{H}_4\}_2\text{O}]$ (**3Hg**)

The ligand $\{2\text{-PPh}_2(\text{O})\text{C}_6\text{H}_5\}_2\text{O}$ (**3**) was synthesized as reported [35]. A reaction between **3** and $\text{Hg}(\text{C}_6\text{F}_5)_2$ was carried out in a 1:1 mole ratio (Scheme 4). Slow evaporation of the solution yielded colorless blocks of complex $[\text{Hg}(\text{C}_6\text{F}_5)_2\{2\text{-PPh}_2(\text{O})\text{C}_6\text{H}_4\}_2\text{O}]$ **3Hg**. This outcome contrasts with the behavior of ligand **1**, which even on a 1:1 stoichiometry, yielded complex **1Hg** in a $2\text{Hg}(\text{C}_6\text{F}_5)_2:1$ ratio. It also contrasts with the behavior of ligand **2** which yields the polymeric complex **2Hg** on this stoichiometry. The $^{19}\text{F}\{^1\text{H}\}$ and $^{31}\text{P}\{^1\text{H}\}$ NMR spectra of **3Hg** are very similar to those of the reactants [23,36] (see ESI, Figures S18 and S19). The IR spectrum of **3Hg** shows strong $\nu(\text{P}=\text{O})$ bands at 1225 and 1165 cm^{-1} , attributable to the free and coordinated $\text{P}=\text{O}$ groups, respectively, where the latter absorption is slightly shifted to longer wavelength from that of the free ligand **3** at 1172 cm^{-1} (owing to the coordination of $\text{P}=\text{O}$ group to mercury) and the former to higher frequencies from the free ligand band at 1216 cm^{-1} (see ESI, Figures S20 and S21). The χ -sensitive mode incorporating C-Hg stretching is located at 806 cm^{-1} and is only slightly shifted from 812 cm^{-1} of free $\text{Hg}(\text{C}_6\text{F}_5)_2$ [5]. This shift is less than observed for **1Hg** and may be the result of the longer (weaker) Hg-O bond in **3Hg** compared to **1Hg**. The carbon-fluorine stretching frequencies at 1069 and 964 cm^{-1} are in a similar region to those of **1Hg**.



Scheme 4. Synthesis of $[\text{Hg}(\text{C}_6\text{F}_5)_2\{2\text{-PPh}_2(\text{O})\text{C}_6\text{H}_4\}_2\text{O}]$ (**3Hg**).

2.8. Molecular Structure of $[\text{Hg}(\text{C}_6\text{F}_5)_2\{2\text{-PPh}_2(\text{O})\text{C}_6\text{H}_4\}_2\text{O}]$ (**3Hg**)

Compound **3Hg** crystallizes in the triclinic space group P-1 (Figure 4). A T-shaped three coordination is observed at the mercury atom. Unlike ligands **1** and **2**, **3** behaves as a monodentate ligand and shows no bridging of the Hg atoms. Only one of the phosphoryl groups is bonded to mercury. The C-Hg-O bond angles around the mercury atom $88.11(15)^\circ$ – $95.62(14)^\circ$ indicate that the T-shape is distorted (Figure 4). The Hg-O bond length (2.711(3) Å) is well within the sum of the Hg and O van der Waals radii [8,27] and is longer than in the bridged bidentate complex **1Hg** but considerably shorter than in the coordination polymer **2Hg**. The P=O bond lengths range between 1.486(3) and 1.493(3) Å. The value for the coordinated P1-O1 is marginally longer than free P2-O3 (Figure 4), but the difference does not meet the three ESD criteria. Investigating the supramolecular interactions in **3Hg** shows C-H...F-H, C-H...C-H and C-H...N interactions along with intermolecular F-C...C- and H...H contacts (Table 4; see also ESI Figures S22 and S23). The C-H...F-C interactions are in the range ~ 2.407 – 2.593 Å with some slightly longer than 2.55 Å [29] (see ESI, Table S4) while the P=O...C contact is 3.191 Å. For all complexes **1Hg**, **2Hg** and **3Hg** the presence of Hg-C bonds leads to Hg...o-F, and Hg...o-C contacts (Table S5) which lie close to the sum of the van der Waals radii [8,27,30].

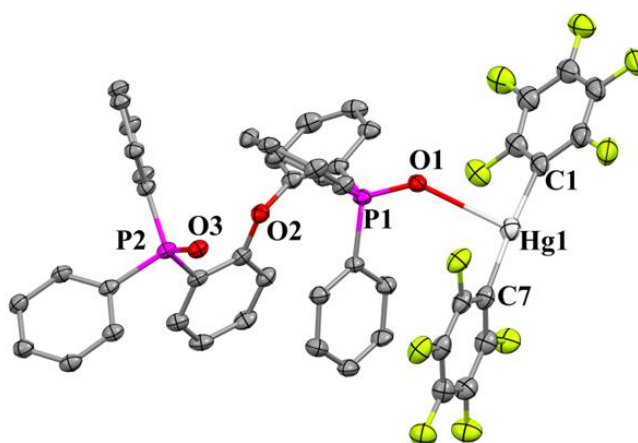


Figure 4. Molecular structure of **3Hg**. All hydrogen atoms are omitted for clarity. Displacement ellipsoids are drawn at the 30% probability level. Selected bond lengths (Å) and bond angles ($^\circ$): Hg1-O1 2.711(3), Hg1-C1 2.070(5), Hg1-C7 2.064(5), P1-O1 1.493(3), P2-O3 1.486(3). C1-Hg1-O1 $88.11(15)$, C7-Hg1-O1 $95.62(14)$, C7-Hg1-C1 $175.15(17)$.

Table 4. Hydrogen-bonds geometry (Å, °) of **3Hg**.

<i>D</i> – <i>H</i> ··· <i>A</i>	<i>D</i> – <i>H</i>	<i>H</i> ··· <i>A</i>	<i>D</i> ··· <i>A</i>	<i>D</i> – <i>H</i> ··· <i>A</i>
C24–H24···F4 [i]	0.93	2.483	3.232	138
C17–H17···F10 [ii]	0.93	2.593	3.423	149
C35–H35···F9 [iii]	0.93	2.407	3.283	157
C45–H45···F9 [iv]	0.93	2.561	3.151	122

[i] 1-*x*, -*y*, 2-*z* [ii] *x*, *y*, *z* [iii] *x*, *y*, *z*, [iv] *x*, *y*, *z*.

3. Conclusions

Complexes of bis(pentafluorophenyl)mercury were prepared with three different bis(phosphane) oxides. Each bisphosphane oxide has a different mode of coordination. Ligand {Ph₂P(O)}₂CH₂ **1** forms complex [Hg(C₆F₅)₂]₂{Ph₂P(O)}₂CH₂ **1Hg** with a single bridging bidentate ligand, whereas ligand {2-PO(NEt₂)₂C₃N₂H₂]₂CH₂ **2** affords the 1D-coordination polymer [Hg(C₆F₅)₂{2-PO(NEt₂)₂C₃N₂H₂]₂CH₂ **2Hg** where each mercury is bound by two bridging bidentate ligands. Further, the bisphosphane oxide (2-PPh₂(O)C₆H₅)₂O **3** coordinates to Hg(C₆F₅)₂ in a monodentate fashion leading to the formation of [Hg(C₆F₅)₂{2-PPh₂(O)C₆H₄]₂O] **3Hg**, a T-shaped monomeric coordination complex. This study on the coordination chemistry of Hg(C₆F₅)₂ reveals there is more to be discovered in the binding of neutral σ-donors to organomercurials, if they are suitably substituted to enhance their acceptor properties.

4. Materials and Methods

4.1. General Considerations

Bis(diphenylphosphano)methane P,P'-dioxide (**1**) [22], bis(2-diphenylphosphanophenyl) ether P,P'-dioxide (**3**) [35], bis(imidazol-1-yl)methane [37], P(NEt₂)₂Cl [38] and [Hg(C₆F₅)₂] [23] were synthesized by literature procedures. Room temperature (25 °C) ¹H, ³¹P{¹H} and ¹³C NMR spectra were recorded with a Bruker DPX 300 instrument using CDCl₃ or CD₃COCD₃ as solvents and resonances were referenced to residual hydrogen-atom or carbon-atom of the deuterated solvent. ³¹P{¹H} NMR spectra are measured with 85% H₃PO₄ as an external standard. Chemical shifts for ¹⁹F{¹H} were referenced externally to trifluorotoluene. Infrared spectra were recorded using a PerkinElmer Spectrum One FT-IR spectrometer (Model no. 73465) in a KBr disk and ATR-Infrared spectra with a PerkinElmer 1600 FT-IR spectrometer from 4000 to 450 cm⁻¹. Elemental analyses (C, H, N) were performed by the School of Chemistry, Monash University.

4.2. Single Crystal X-ray Structure Determination

Crystals for X-ray structure analysis were grown using saturated solutions in hexane (**2**), acetonitrile (**1Hg**), acetonitrile: dichloromethane (**2Hg**) or chloroform (**3Hg**). Crystals **2**, **1Hg**, **2Hg** and **3Hg** were immersed in Paratone, and were measured on a Rigaku Saturn724 diffractometer (**2**), a Rigaku SynergyS diffractometer (**1Hg**) and the MX1 beamlines at the Australian Synchrotron (**2Hg** and **3Hg**). The Saturn724 was operated using microsource Mo Kα radiation (λ = 0.71073 Å) at 150 K, the SynergyS was operated using microsource Mo Kα radiation (λ = 0.71073 Å) at 123 K, and the MX1 beamline was operated using a single wavelength (λ = 0.71073 Å) at 100K. Data processing was conducted using the CrysAlisPro.55 software suite [39]. Structural solutions were obtained by ShelXT [40] and refined using full-matrix least-squares methods against F₂ using SHELXL [41], in conjunction with the Olex2 [42] graphical user interface. All hydrogen atoms were placed in calculated positions using the riding model. Crystal and refinement data are given in Table 5.

Table 5. Crystallographic Data.

Compound	2	1Hg	2Hg	3Hg
Empirical formula	C ₂₃ H ₄₆ N ₈ O ₂ P ₂	[C ₄₉ H ₂₂ F ₂₀ Hg ₂ O ₂ P ₂]	[C ₃₅ H ₄₆ F ₁₀ HgN ₈ O ₂ P ₂]	[C ₄₈ H ₂₈ F ₁₀ HgO ₃ P ₂]
Formula weight	528.62	1485.78	1063.33	1105.23
Temperature/K	150	123	100	100
Crystal system	Monoclinic	Monoclinic	Triclinic	Triclinic
Space group	P2 ₁ /n	C2/c	P-1	P-1
a/Å	9.3556(3)	14.0695(2)	11.480(2)	8.510(17)
b/Å	12.0193(4)	17.0277(3)	12.900(3)	11.680(2)
c/Å	25.8957(8)	19.1180(3)	15.330(3)	21.020(4)
α/°	90	90	110.03(3)	84.47(3)
β/°	94.663(3)	92.6470(10)	97.81(3)	85.62(3)
γ/°	90	90	95.36(3)	83.13(3)
Volume/Å ³	2902.28(16)	4575.24(13)	2089.2(8)	2060.2(7)
Z	4	4	2	2
ρ _{calc} /cm ³	1.210	2.157	1.690	1.782
μ/mm ⁻¹	0.184	6.897	3.847	3.903
F(000)	1144.0	2808.0	1056.0	1080.0
Mo Kα	Mo Kα (λ = 0.71073)	Mo Kα (λ = 0.71073)	Synchrotron (λ = 0.71073)	Mo Kα (λ = 0.71073)
radiation/Synchrotron, λ/Å	Mo Kα (λ = 0.71073)	Mo Kα (λ = 0.71073)	Synchrotron (λ = 0.71073)	Mo Kα (λ = 0.71073)
Crystal size/mm ³	0.258 × 0.115 × 0.085	0.076 × 0.064 × 0.03	0.089 × 0.068 × 0.056	0.1 × 0.1 × 0.08
2θ range for datacollection/°	4.764 to 67.282	7.038 to 63.782	2.874 to 50.696	1.95 to 58.188
Reflections collected	32458	29404	37445	41307
Independent reflections	9353	6548	7572	8939
Data/restraints/parameters	9353/27/382	6548/0/383	7572/228/711	8942/0/577
Goodness-of-fit on F ²	1.018	1.035	1.068	1.060
R ₁ [a]	0.0481	0.0193	0.0372	0.0376
wR ₂ [b]	0.1287	0.0434	0.0965	0.1078

4.3. Experimental Section

4.3.1. Synthesis of {PO(NEt₂)₂C₃N₂H₂}₂CH₂ (2)

To a solution of bis(imidazol-1-yl)methane (0.507 g, 3.42 mmol) dissolved in dry THF (50 mL) was added n BuLi (1.6 M solution in hexane, 7.5 mmol, 4.6 mL) dropwise at -78 °C under nitrogen using Schlenk-line techniques and the reaction mixture was slowly warmed to room temperature followed by stirring for 2 h. P(NEt₂)₂Cl (1.570 g, 7.5 mmol) in THF (20 mL) was added dropwise at -78 °C and the reaction mixture was slowly allowed to reach room temperature and was further stirred for 12 h. The solvent was removed under vacuum and the resulting crude diphosphane was given an aqueous work-up and extracted with dichloromethane. The crude diphosphane was dissolved in THF and 30% H₂O₂ (5.9 mmol, 0.70 mL) was added to the solution of diphosphane at 0 °C and stirred for 1 h. The reaction mixture was evaporated under reduced pressure giving a yellow-colored viscous liquid. The viscous liquid obtained was dissolved in a minimum amount of hexane and kept at -20 °C for 24 h to yield colorless blocks of **2**. Yield = 362 mg (20%) FT-IR (KBr disc cm⁻¹) 3104 (s, br), 2975 (vs), 2942 (m), 2879 (s), 1743 (s), 1669 (s, vbr), 1514 (w), 1471 (s), 1388 (s), 1363 (s), 1285 (s, br), 1262 (s, br), 1220 (m, br), 1212 (s, br), 1202 (m, br), 1110 (s), 1062 (s), 1025 (vs), 951 (vs), 936 (m), 792 (vs), 769 (w), 711 (s), 691 (s), 666 (s), 562 (vs, br), 552 (m, br), 531 (m, br). ¹H NMR (500 MHz, CDCl₃) δ 8.05 (s, 2H), 7.16 (d, *J* = 2.4 Hz, 2H), 7.10 (s, 2H), 3.27–3.03 (m, 16H), 1.04 (s, 24H). ³¹P {¹H} NMR (202 MHz, CDCl₃) δ 15.95. ¹³C NMR (126 MHz, CDCl₃) δ 141.32, 139.68, 130.06, 129.92, 124.00, 123.97, 54.86, 38.60, 38.56.

4.3.2. Synthesis of [{Hg(C₆F₅)₂]₂(Ph₂P(O))₂CH₂] (1Hg)

Hg(C₆F₅)₂ (49.2 mg, 0.092 mmol) and **1** (19.2 mg, 0.046 mmol) were stirred together in acetonitrile (10 mL). Slow evaporation of acetonitrile solution yielded colorless blocks of **1Hg**. Yield 65 mg (95%), ³¹P {¹H} NMR (162 MHz, *d*₆-Acetone) δ 23.13. ¹⁹F {¹H} NMR (377 MHz, *d*₆-Acetone) δ -119.9 (³*J*_{F,Hg} = 449 Hz, 4F), -155.7 (2F), -162.2 (4F, ⁴*J*_{F,Hg} = 136 Hz). FT-IR (ATR cm⁻¹): 2923 (w, br), 2362 (w, br), 1638 (s,w), 1506 (s), 1473 (vs), 1435 (s), 1368 (s), 1270 (w), 1181 (vs), 1119 (s), 1100 (w), 1055 (s), 999 (w, br), 957 (vs), 794 (s), 744 (m), 730 (s), 691

(vs). Elemental analysis Calcd (%) for $C_{49}H_{22}F_{20}Hg O_2P_2$: C 39.61, H 1.49; found C 39.35, H 1.32.

4.3.3. Synthesis of $[Hg(C_6F_5)_2\{2-PO(NEt_2)_2C_3N_2H_2\}_2CH_2]_n$ (**2Hg**)

$Hg(C_6F_5)_2$ (49.2 mg, 0.092 mmol) and **2** (25 mg, 0.046 mmol) were stirred together in $CHCl_3$ (5 mL). The slow evaporation of the chloroform solution yielded colorless blocks of **2Hg** in an amount sufficient for structure determination. Half of the $Hg(C_6F_5)_2$ remained unreacted.

4.3.4. Synthesis of $[Hg(C_6F_5)_2\{PPh_2(O)C_6H_4\}_2O]$ (**3Hg**)

$Hg(C_6F_5)_2$ (24.6 mg, 0.046 mmol) and **3** (26.25 mg, 0.046 mmol) were stirred together in $CHCl_3$ (5 mL). Slow evaporation of chloroform solution yielded colorless blocks of **3Hg**. Yield = 45 mg (88%). $^{31}P\{^1H\}$ NMR (162 MHz, $CDCl_3$) δ 25.93. $^{19}F\{^1H\}$ NMR (377 MHz, $CDCl_3$) δ -119.43 (4F, $^3J_{F,Hg} = 417$ Hz), -150.34 (2F), -158.79 (4F, $^4J_{F,Hg} = 122$ Hz). FT-IR (KBr disc cm^{-1}): Overall broad feature at 3058 (s), 2930(m), and 2860(w), 1642 (vs), 1596 (vs), 1567 (vs), 1512 (s), 1478 (vs), 1439 (vs, br), 1310 (m), 1272 (m), 1271 (m), 1225 (vs), 1203 (m), 1186 (w), 1165 (vs), 1133 (w), 1122 (vs), 1081 (vs), 1069 (vs), 997 (m), 964 (vs), 878 (s), 806 (vs), 759 (s), 731 (s), 697 (s), 610 (m), 584 (m), 539 (vs), 518 (vs), 490 (w).

Supplementary Materials: The following supporting information can be downloaded at: <https://www.mdpi.com/article/10.3390/cryst13030530/s1>, including NMR spectra, additional experimental, X-ray and refinement data, bond lengths and angle data.

Author Contributions: Conceptualization, G.B.D. and V.L.B.; synthesis, spectroscopy, characterization, original draft, S.R.; X-ray crystallography, O.A.B. and Z.G.; supervision and editing, M.S.B.; supervision, rewriting, editing, G.B.D. and V.L.B. All authors have read and agreed to the published version of the manuscript.

Funding: GBD and VLB gratefully acknowledges the Australian Research Council (ARC) for funding, DP190100798 and FT200100918, respectively.

Data Availability Statement: Crystal data can be obtained free of charge from The Cambridge Crystallographic Data Centre: CCDC 2243139–2243142 for compounds **2**, **1Hg**, **2Hg** and **3Hg**, respectively.

Acknowledgments: We are grateful to the Faculty of Science, Monash University and the Department of Chemistry, the Indian Institute of Technology, Bombay, for providing the required facility for carrying out the work. SR gratefully acknowledges the Indian Institute of Technology Bombay-Monash Academy for the financial support. We thank Craig Forsyth and Dipanjan Mondal for X-ray crystallography assistance.

Conflicts of Interest: The authors declare no conflict of interest.

References

1. Chambers, R.D.; Coates, G.E.; Livingstone, J.G.; Musgrave, W.K.R. 847. The preparation and study of some pentafluorophenylmercury compounds. *J. Chem. Soc.* **1962**, 4367–4371. [[CrossRef](#)]
2. Lin, T.-P.; Nelson, R.C.; Wu, T.; Miller, J.T.; Gabbai, F.P. Lewis acid enhancement by juxtaposition with an onium ion: The case of a mercury stibonium complex. *Chem. Sci.* **2012**, *3*, 1128–1136. [[CrossRef](#)]
3. Canty, A.; Gatehouse, B. The crystal structures of disordered crystals of adducts of diphenylmercury with bidentate ligands. *Acta Crystallogr. B* **1972**, *28*, 1872–1888. [[CrossRef](#)]
4. Korpar-Cölig, B.; Popović, Z.; Bruvo, M.; Vicković, I. Addition compounds of bis(trifluoromethyl)mercury with tetraphenylphosphonium and tetraphenylarsonium halides and thiocyanates. *Inorg. Chim. Acta* **1988**, *150*, 113–118. [[CrossRef](#)]
5. Connett, J.; Davies, A.G.; Deacon, G.; Green, J. Organomercury compounds. Part I. Mercury pentafluorobenzoates and their decarboxylation to pentafluorophenylmercury compounds. *J. Chem. Soc. C* **1966**, 106–111. [[CrossRef](#)]
6. Canty, A.; Deacon, G. Organomercury compounds. XI. Some coordination derivatives of bis(pentafluorophenyl)mercury. *Aust. J. Chem.* **1971**, *24*, 489–499. [[CrossRef](#)]
7. Canty, A.J.; Gatehouse, B.M. Crystal structure of tetrakis(pentafluorophenyl)- μ -bis(diphenylarsinomethane)-dimercury(II), a three-coordinate mercury complex. *J. Chem. Soc. D* **1971**, 443–444. [[CrossRef](#)]
8. Canty, A.J.; Deacon, G.B. The van der Waals radius of mercury. *Inorg. Chim. Acta* **1980**, *45*, L225–L227. [[CrossRef](#)]

9. Schulz, F.; Pantenburg, I.; Naumann, D. Synthesen und Strukturen von Perfluororganohalogenomercuraten $[\text{Hg}(\text{R}_f)_2\text{X}]$ —($\text{R}_f = \text{CF}_3, \text{C}_6\text{F}_5$; $\text{X} = \text{Br}, \text{I}$). *Z. Anorg. Allg. Chem.* **2003**, *629*, 2312–2316. [[CrossRef](#)]
10. Naumann, D.; Schulz, F. Strukturen von neuen Bis(pentafluorophenyl)halogenomercuraten $[\{\text{Hg}(\text{C}_6\text{F}_5)_2\}_3(\mu\text{-X})]$ —($\text{X} = \text{Cl}, \text{Br}, \text{I}$). *Z. Anorg. Allg. Chem.* **2005**, *631*, 715–718. [[CrossRef](#)]
11. Burrell, C.N.; Bodine, M.I.; Elbjeirami, O.; Reibenspies, J.H.; Omary, M.A.; Gabbai, F.P. Enhancement of external spin–orbit coupling effects caused by metal–metal cooperativity. *Inorg. Chem.* **2007**, *46*, 1388–1395. [[CrossRef](#)] [[PubMed](#)]
12. Deacon, G.B.; Forsyth, C.M.; Junk, P.C.; Ness, T.J.; Izgorodina, E.; Baldamus, J.; Meyer, G.; Pantenburg, I.; Hitzbleck, J.; Ruhlandt-Senge, K. The Supramolecular Architecture of Arene Complexes of Bis(polyfluorophenyl)mercurials. *Eur. J. Inorg. Chem.* **2008**, *2008*, 4770–4780. [[CrossRef](#)]
13. Kim, M.; Taylor, T.J.; Gabbai, F.P. $\text{Hg}(\text{II})\cdots\text{Pd}(\text{II})$ metallophilic interactions. *J. Am. Chem. Soc.* **2008**, *130*, 6332–6333. [[CrossRef](#)]
14. Tsunoda, M.; Fleischmann, M.; Jones, J.S.; Bhuvanesh, N.; Scheer, M.; Gabbai, F.P. Supramolecular aggregation of Ni(salen) with $(\text{C}_6\text{F}_5)_2\text{Hg}$ and $[\text{o-C}_6\text{F}_4\text{Hg}]_3$. *Dalton Trans.* **2016**, *45*, 5045–5051. [[CrossRef](#)]
15. López-de-Luzuriaga, J.M.; Monge, M.; Olmos, M.E.; Pascual, D.; Lasanta, T. Amalgamating at the molecular level. A study of the strong closed-shell $\text{Au}(\text{i})\cdots\text{Hg}(\text{ii})$ interaction. *Chem. Commun.* **2011**, *47*, 6795–6797. [[CrossRef](#)] [[PubMed](#)]
16. Lasanta, T.; López-de-Luzuriaga, J.M.; Monge, M.; Olmos, M.E.; Pascual, D. Experimental and Theoretical Evidence of the Existence of Gold(I)–Mercury(II) Interactions in Solution through Fluorescence-Quenching Measurements. *Chem. Eur. J.* **2013**, *19*, 4754–4766. [[CrossRef](#)]
17. Rosario-Amorin, D.; Dehaut, J.P.; Caudle, L.J.; Dickie, D.A.; Paine, R.T. Synthesis and molecular structures of mercury(II) complexes of carbamoylmethylphosphoryl ligands. *Phosphorus Sulfur Silicon Relat. Elem.* **2016**, *191*, 520–526. [[CrossRef](#)]
18. Tikhonova, I.A.; Dolgushin, F.M.; Tugashov, K.I.; Petrovskii, P.V.; Furin, G.G.; Shur, V.B. Coordination chemistry of polymercuramacrocycles. Complexation of cyclic trimeric perfluoro-o-phenylenemercury with neutral oxygenous Lewis bases. *J. Organomet. Chem.* **2002**, *654*, 123–131. [[CrossRef](#)]
19. Olaru, M.; Krupke, S.; Lork, E.; Mebs, S.; Beckmann, J. Transmetalation of bis(6-diphenylphosphinoxy-acenaphth-5-yl)mercury with tin tetrachloride, antimony trichloride and bismuth trichloride. *Dalton Trans.* **2019**, *48*, 5585–5594. [[CrossRef](#)]
20. Cole, M.L.; Deacon, G.B.; Junk, P.C.; Konstas, K.; Roesky, P.W. Novel Mercury Phosphanylamides. *Eur. J. Inorg. Chem.* **2005**, *2005*, 1090–1098. [[CrossRef](#)]
21. Padron, D.A.; Klausmeyer, K.K. Syntheses and coordination studies of 2-(diphenylphosphinomethyl)pyridine and its oxide towards mercury(II). *Polyhedron* **2012**, *34*, 215–220. [[CrossRef](#)]
22. Aslandukov, A.N.; Utochnikova, V.V.; Goriachiy, D.O.; Vashchenko, A.A.; Tsymbarenko, D.M.; Hoffmann, M.; Pietraszkiewicz, M.; Kuzmina, N.P. The development of a new approach toward lanthanide-based OLED fabrication: New host materials for Tb-based emitters. *Dalton Trans.* **2018**, *47*, 16350–16357. [[CrossRef](#)]
23. Deacon, G.B.; Cosgriff, J.E.; Lawrenz, E.T.; Forsyth, C.M.; Wilkinson, D.L. Section 2.3: Organolanthanide(II) Complexes in Lanthanides and Actinides. In *Synthetic Methods of Organometallic and Inorganic Chemistry*; Edelman, F.T., Herrmann, W.A., Eds.; Georg Thieme Verlag: Stuttgart, Germany; New York, NY, USA, 1997; Volume 6, p. 48.
24. Rangarajan, S.; Beaumont, O.A.; Balakrishna, M.S.; Deacon, G.B.; Blair, V.L. Synthesis and Characterisation of Novel Bis(diphenylphosphane oxide)methanidoytterbium(III) Complexes. *Molecules* **2022**, *27*, 7704. [[CrossRef](#)] [[PubMed](#)]
25. Deacon, G.B.; Green, J.H.S. Vibrational spectra of ligands and complexes—VI: Infrared spectra of triphenylarsine, triphenylarsine oxide, and triphenylphosphine oxide complexes. *Spectrochim. Acta A Mol. Spectrosc.* **1969**, *25*, 355–364. [[CrossRef](#)]
26. Guo, Z.; Huo, R.; Tan, Y.Q.; Flosbach, N.T.; Wang, N.; Leonhardt, C.; Urbatsch, A.; Deacon, G.B.; Junk, P.C.; Izgorodina, E.I.; et al. A new twist on an old molecule: A rotameric isomer of bis(pentafluorophenyl)mercury. *J. Coord. Chem.* **2021**, *74*, 2947–2958. [[CrossRef](#)]
27. Nyburg, S.C.; Faerman, C.H. A revision of van der Waals atomic radii for molecular crystals: N, O, F, S, Cl, Se, Br and I bonded to carbon. *Acta Crystallogr. B Struct.* **1985**, *41*, 274–279. [[CrossRef](#)]
28. Grachova, E.; Linti, G.; Vologzhanina, A. CCDC 877465: EBIXEV Experimental Crystal Structure Determination. In *CSD Communications*; University of Cambridge: Cambridge, UK, 2016.
29. Dunitz, J.D.; Taylor, R. Organic Fluorine Hardly Ever Accepts Hydrogen Bonds. *Chem. Eur. J.* **1997**, *3*, 89–98. [[CrossRef](#)]
30. Bondi, A. van der Waals volumes and radii. *J. Phys. Chem.* **1964**, *68*, 441–451. [[CrossRef](#)]
31. Antiñolo, A.; Carrillo-Hermosilla, F.; Díez-Barra, E.; Fernández-Baeza, J.; Fernández-López, M.; Lara-Sánchez, A.; Moreno, A.; Otero, A.; María Rodríguez, A.; Tejada, J. New functionalized bis(pyrazol-1-yl)methane ligands. Synthesis, spectroscopic characterization of early and late transition metal complexes containing a functionalized N,N or P,P-chelate bis(5-diphenylphosphinopyrazol-1-yl)methane ligand. *J. Chem. Soc. Dalton Trans.* **1998**, 3737–3744. [[CrossRef](#)]
32. Bhat, S.A.; Mague, J.T.; Balakrishna, M.S. Gold(i) complexes of bisphosphines with bis(azol-1-yl)methane backbone: Structure of a rare dinuclear gold(i) complex $[(\text{Au}_2\text{Cl})\{\text{CH}_2(1,2\text{-C}_3\text{H}_2\text{N}_2\text{PPh}_2)_2\}_3\text{Cl}]$. *Dalton Trans.* **2015**, *44*, 17696–17703. [[CrossRef](#)]
33. Bhat, S.A.; Sonawane, S.C.; Mague, J.T.; Balakrishna, M.S. Synthesis and characterization of Mo(0) and W(0) complexes of bis(azol-1-yl)methane based bisphosphines. *J. Coord. Chem.* **2021**, *74*, 2253–2262. [[CrossRef](#)]
34. Geiger, D.K.; DeStefano, M.R. Conformational differences and intermolecular C–H...N interactions in three polymorphs of a bis(pyridinyl)-substituted benzimidazole. *Acta Cryst. C* **2016**, *72*, 867–874. [[CrossRef](#)]

35. Pietraszkiewicz, M.; Mal, S.; Pietraszkiewicz, O.; Górski, K.; Chelwani, N. Photoluminescent Tetrazolate-based Eu(III) Complexes: An Outstanding Impact of Aromatic Phosphine Oxide Co-ligands on the Photoluminescence Quantum Yields. *Z Naturforsch.* **2014**, *69*, 239–247. [[CrossRef](#)]
36. Li, Y.; Lu, L.-Q.; Das, S.; Pisiewicz, S.; Junge, K.; Beller, M. Highly Chemoselective Metal-Free Reduction of Phosphine Oxides to Phosphines. *J. Am. Chem. Soc.* **2012**, *134*, 18325–18329. [[CrossRef](#)] [[PubMed](#)]
37. Díez-Barra, E.; de la Hoz, A.; Sánchez-Migallón, A.; Juan, T. Phase Transfer Catalysis without Solvent. Synthesis of Bisazolyalkanes. *Heterocycles* **1992**, *34*, 1365–1373. [[CrossRef](#)]
38. Qin, L.; Ren, X.; Lu, Y.; Li, Y.; Zhou, J. Intermolecular Mizoroki–Heck Reaction of Aliphatic Olefins with High Selectivity for Substitution at the Internal Position. *Angew. Chem. Int. Ed.* **2012**, *51*, 5915–5919. [[CrossRef](#)]
39. Agilent Technologies Ltd. *CrysAlisPRO, Version 39*; Agilent Technologies Ltd.: Yarnton, UK, 2021.
40. Sheldrick, G. SHELXT—Integrated space-group and crystal-structure determination. *Acta Cryst. A* **2015**, *71*, 3–8. [[CrossRef](#)] [[PubMed](#)]
41. Sheldrick, G. Crystal structure refinement with SHELXL. *Acta Cryst. C* **2015**, *71*, 3–8. [[CrossRef](#)] [[PubMed](#)]
42. Dolomanov, O.V.; Bourhis, L.J.; Gildea, R.J.; Howard, J.A.K.; Puschmann, H. OLEX2: A complete structure solution, refinement and analysis program. *J. Appl. Cryst.* **2009**, *42*, 339–341. [[CrossRef](#)]

Disclaimer/Publisher’s Note: The statements, opinions and data contained in all publications are solely those of the individual author(s) and contributor(s) and not of MDPI and/or the editor(s). MDPI and/or the editor(s) disclaim responsibility for any injury to people or property resulting from any ideas, methods, instructions or products referred to in the content.